The Plant Cell, Vol. 11, 57–68, January 1999, www.plantcell.org © 1999 American Society of Plant Physiologists

Mutations in the Arabidopsis Gene *IMMUTANS* Cause a Variegated Phenotype by Inactivating a Chloroplast Terminal Oxidase Associated with Phytoene Desaturation

Pierre Carol,[a,1,2] David Stevenson,[b,1,3] Cordelia Bisanz,[a] Jürgen Breitenbach,[c] Gerhard Sandmann,[c] Regis Mache,[a] George Coupland,[b] and Marcel Kuntz[a]

[a] Laboratoire de Génétique Moléculaire des Plantes, Université Joseph Fourier, CNRS UMR 5575, BP 53X, 38041 Grenoble Cedex 09, France

[b] Department of Molecular Genetics, John Innes Centre, Colney Lane, Norwich, NR4 7UH, United Kingdom

[c] Photosynthesis Group, Botanical Institute, Goethe-Universität, Frankfurt, Germany

The *immutans* (*im*) mutant of Arabidopsis shows a variegated phenotype comprising albino and green somatic sectors. We have cloned the *IM* gene by transposon tagging and show that even stable null alleles give rise to a variegated phenotype. The gene product has amino acid similarity to the mitochondrial alternative oxidase. We show that the IM protein is synthesized as a precursor polypeptide that is imported into chloroplasts and inserted into the thylakoid membrane. The albino sectors of *im* plants contain reduced levels of carotenoids and increased levels of the carotenoid precursor phytoene. The data presented here are consistent with a role for the IM protein as a cofactor for carotenoid desaturation. The suggested terminal oxidase function of IM appears to be essential to prevent photooxidative damage during early steps of chloroplast formation. We propose a model in which IM function is linked to phytoene desaturation and, possibly, to the respiratory activity of the chloroplast.

INTRODUCTION

In plant cells, plastid differentiation is intimately linked to organogenesis and is affected by both developmental regulatory mechanisms and environmental conditions. The complex mechanisms involved in the phototransformation of the plastids of dark-grown seedlings (etioplasts) to photosynthetically active plastids (chloroplasts) have been described extensively (reviewed in Mullet, 1988; Taylor, 1989; Chory and Susek, 1994). Alternatively, developing grass tissues provide a unique system in which a gradient of developmental stages of cells and plastids (proplastids to chloroplasts) is present (Mullet, 1988; Bilang and Bogorad, 1996; Inada et al., 1996).

Mutants visibly impaired in chloroplast differentiation can be selected by their pale green, yellow, or albino color. The chlorophyll-deficient mutant *olive* of Antirrhinum has this phenotype (Hudson et al., 1993). Not all of these mutants are altered directly in pigment synthesis. Putative functions can be proposed for mutated genes based on the similarity of their coding sequences to known proteins. The Arabidopsis mutant *albino3* (Sundberg et al., 1997) is impaired in chloroplast membrane biogenesis, as suggested by amino acid sequence similarity between ALBINO3 and the yeast mitochondrial OXA1 protein involved in mitochondrial biogenesis. The Arabidopsis *cla1* mutation (Mandel et al., 1996) identifies an enzyme also present in cyanobacteria. Mutations also have been described that affect the proplastid-to-chloroplast transition. The *dag* mutant from Antirrhinum (Chatterjee et al., 1996) and *dcl1* from tomato (Keddie et al., 1996) do not contain chloroplasts but rather plastids resembling nondifferentiated proplastids. These genes together with the *PALE CRESS* gene from Arabidopsis (Reiter et al., 1994) affect both chloroplast development and leaf architecture.

One class of mutations gives rise to variegated plants that have a mutant phenotype in some sectors and a wild-type phenotype in others. The *iojap* (Han et al., 1992) mutant of maize or the chloroplast mutator in maize and Arabidopsis (Martínez-Zapater et al., 1992) all have a variegated albino phenotype similar to heteroplastid tobacco plants created after selection for chloroplast mutations. They seem to affect chloroplast function or genome expression during plant development. Although *chloroplast mutator* affects the mitochondrial genome, it interacts with chloroplast development because its effect is visible on chloroplasts (Martínez-Zapater et al., 1992; Sakamoto et al., 1996).

[1] These authors contributed equally to this work.

[2] To whom correspondence should be addressed. E-mail pierre.carol@UJF-grenoble.fr; fax 33-4-76-51-43-36.

[3] Current address: IACR–Long Ashton Research Station, Long Ashton, Bristol, BS18 9AF, UK.

Albino mutants are of particular interest because, unlike other leaf color mutants, they are devoid of carotenoid pigments. Carotenoids are a diverse group of pigments that function as accessory pigments during light harvesting and are integral and structural components of the photosynthetic apparatus (reviewed in Bramley, 1997). Carotenoids also are involved in photoprotection by quenching singlet oxygen and other reactive species. After excitation by light, chlorophyll (triplet state) can transfer its energy to molecular oxygen, and the resulting singlet oxygen can cause oxidative damage. Carotenoids take up energy from singlet oxygen and dissipate it as heat.

In plants, carotenoids are synthesized exclusively in plastids from the colorless C40 backbone, phytoene, which is subjected to sequential desaturation reactions. In plants, the first two of these reactions are catalyzed by phytoene desaturase (PDS) to form phytofluene and then ζ-carotene (Bartley et al., 1991), whereas the next two desaturation reactions are catalyzed by ζ-carotene desaturase to form neurosporene and then lycopene (Albrecht et al., 1995). Lycopene is cyclized to form either α- or β-carotene, which can be subjected to oxidation reactions to produce xanthophylls present in photosynthetic tissues.

Mutants devoid of the α-carotene–derived xanthophyll lutein are viable and were selected by an HPLC screen (Pogson et al., 1996). Mutants in the β-carotene–derived xanthophylls (e.g., impaired in zeaxanthin epoxidase) could be selected because of their deficiency in abscisic acid (Marin et al., 1996). Most of the mutations leading to the accumulation of early intermediates of the pathway are expected to be lethal due to the lack of protection against photooxidation. However, variegated mutants (green/white) can survive because the green tissue provides enough photosynthesis for plant growth and reproduction, allowing the propagation of homozygous mutant plants and thereby permitting the study of chloroplast-deficient (containing white plastids) living tissues.

A striking example of such a variegated phenotype is provided by the *immutans* (*im*) mutant from Arabidopsis (Wetzel et al., 1994). This mutant shows a light-dependent variegated phenotype. Light affects the phenotype of the *im* mutant by increasing the amount of albino tissue in the mutant. The phenotype is cell autonomous because once sectors have acquired their respective phenotypes, they do not revert, and there are clear boundaries between sectors. Whether the defect is linked to pigment (carotenoid) biosynthesis or involves a regulatory mechanism is not known.

We are interested in the mechanisms controlling plastid differentiation and carotenoid biosynthesis and the relationship between both processes. We have been using transposon mutagenesis to isolate transposon-tagged alleles of mutations affecting chloroplast development or function. For the reasons mentioned above, we have studied a variegated albino mutant. This mutant was found to identify the *IM* locus. The corresponding gene and cDNA were isolated. We propose that the IM protein acts as a cofactor for phytoene desaturation and as a terminal oxidase. Its role in chloroplast formation also is discussed.

RESULTS

Identification of a Transposon-Induced Allele of *im*

A transposon mutagenesis experiment was performed to produce albino Arabidopsis mutants, with the goal of characterizing nuclear genes involved in chloroplast function and development. The Arabidopsis line carrying Tn*113* harbors a T-DNA insertion on chromosome 4 carrying *Ds(Hyg)*, a modified *Dissociation* transposable element conferring resistance to hygromycin (Long et al., 1997). This line was crossed with a line carrying the *Activator* (*Ac*) transposase coding sequence under the control of the constitutive cauliflower mosaic virus 35S promoter (35S::*TPase*) to activate *Ds(Hyg)* transposition (Coupland, 1992; Long et al., 1993, 1997). From the progeny of the Tn*113 Ds(Hyg)* 35S::*TPase*–containing line, 300 independent plants were selected for excision followed by reinsertion of the *Ds(Hyg)* element. One line was studied further because some of its progeny showed an albino phenotype when grown in vitro on agar-containing medium.

When the progeny of a plant that was heterozygous for the albino mutation were grown in the greenhouse, we observed albino plants that developed green sectors of the wild-type phenotype. We also observed plants with this phenotype that were grown in vitro on agar-containing medium (Figure 1A). Although mutations caused by transposon insertion often give rise to variegated phenotypes due to transposon excision in somatic sectors, excision of the *Ds(Hyg)* element could not explain this variegated phenotype because mutant plants that lacked the *Ac* transposase gene, which is essential for *Ds(Hyg)* excision, also appeared variegated.

When green sectors encompassed the meristem, they gave rise to fertile floral stems. When seeds from green sectors were sown, a variety of variegated plants germinated and developed, suggesting that the green phenotype is not caused by a reversion of the mutation (Figure 1A). This phenotype is reminiscent of the *im*-conferred phenotype that was described previously as a chloroplast autonomous mutation (Rédei, 1963; Wetzel et al., 1994).

The white tissues of *im* have been shown to lack functional carotenoid and to accumulate phytoene, which is an intermediate compound of the carotenoid biosynthesis pathway. We analyzed the carotenoid content of the variegated albino and compared it with the wild type (Figure 1B). Samples of white tissues or variegated or green tissues were analyzed. All samples were taken from the descendants of the same heterozygous plant. The wild-type leaves exhibited a typical composition of colored carotenoids with a content of 1.6 ± 0.29 mg/g dry weight. Of these, ~50%

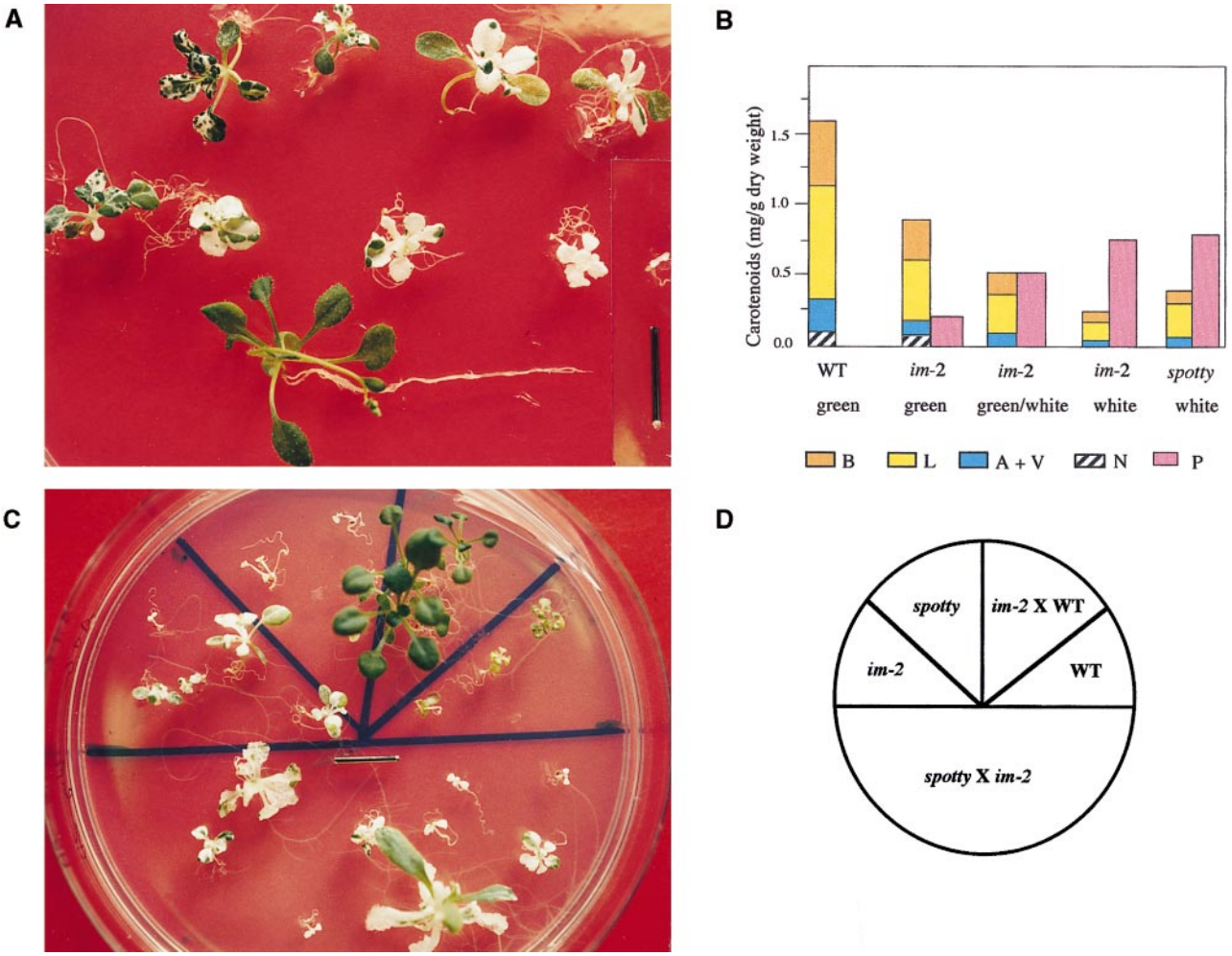

Figure 1. The *Ds(Hyg)*-Tagged Mutants Have a Variegated Phenotype and Are Blocked in Carotenoid Biosynthesis.

(A) When planted on agar medium, mutants show a variable phenotype, ranging from albino to variegated. Top row, variegated progeny of a heterozygous plant. Bottom row, wild-type control grown under the same conditions. Bar = 1 cm.

(B) Accumulation of colored carotenoids and phytoene in Arabidopsis leaves. WT green, leaves from the wild type; *im-2* green, green leaves taken from green-sectored mutants; *im-2* green/white, variegated leaves from mutant plants; *im-2* white, white tissues from mutant plants; *spotty* white, white tissue from *im* (*spotty* allele). B, β-carotene; L, lutein; A, antheraxanthin; V, violaxanthin; N, neoxanthin; P, phytoene.

(C) Allelism test between an *im-2 Ds(Hyg)*–tagged variegated mutant and *im* (the recessive *spotty* allele; Wetzel et al., 1994). F_1 seeds from different crosses were planted on a hygromycin-containing medium to select for the presence of *Ds(Hyg).*

(D) Schematic view of the plate shown in **(C)**. Hygromycin-resistant plants (containing *Ds[Hyg]*) are resistant. *im spotty* and wild-type (WT) plants are sensitive to hygromycin. Heterozygous F_1 plants from *im*-2 crossed to wild type have the wild-type phenotype and are resistant to hygromycin. Because F_1 seeds from the cross between *im* and *im-2* have the mutant phenotype, both mutations are allelic and identify the same locus. Because F_1 seeds from the cross between *im-2* and wild-type plants are of the wild-type phenotype, *im-2* is a recessive mutant allele of *IM.*

was lutein and almost 30% was β-carotene. The β-carotene–derived xanthophylls violaxanthin (~10%), antheraxanthin (~5%), and neoxanthin (~5%) also were identified. The colorless phytoene was below the detection limit. Green leaves of the mutant contained approximately half of the colored carotenoids of the control, and substantial amounts of phytoene were found (Figure 1B). The content of colored carotenoids decreased further in variegated (green/white) and totally white leaves, whereas increasing amounts of phytoene were observed concurrently. However, the accumulation of phytoene did not compensate fully for the decrease in colored carotenoids, as compared with the control.

This is not unexpected because a portion of the carotenoids, including phytoene, are likely to be destroyed by photooxidation (see Discussion) together with the chlorophylls.

The carotenoid composition, including phytoene, in white tissues from the variegated albino was very similar to that found in the white *im* material. The relative percentage of distribution of individual colored carotenoids was consistent in all samples analyzed (Figure 1B). We conclude that the mutation described here affects the carotenoid biosynthetic pathway directly or indirectly at the level of the reaction catalyzed by the PDS enzyme.

Allelism tests between *im* (the *spotty* allele; described in Wetzel et al., 1994) and the variegated albino identified in this study proved that both mutations are allelic, hence identifying the same locus (Figures 1C and 1D). We deduced from these data that we identified a new, possibly tagged, allele of *im.* We refer to it as *im-2.*

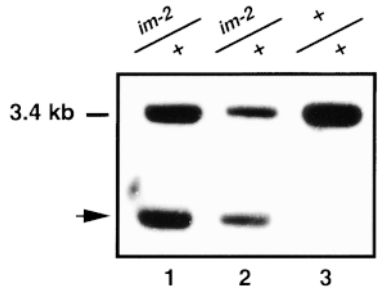

Figure 2. *Ds(Hyg)* Is Inserted in the *IM* Gene.

A gel blot shows an extra fragment in Arabidopsis lines carrying the *im-2* mutation. DNA extracted from heterozygous plants (*im-2*/+) (lanes 1 and 2) or plants with a wild-type genotype (lane 3; +/+) was digested with EcoRI, transferred to a nylon membrane, and probed with the *Ds(Hyg)* flanking sequence. A 3.4-kb fragment is revealed in all three genotypes corresponding to the wild-type allele of *IM.* The band present only in plants carrying *im-2* (arrow) reveals the interruption of *IM* in *Ds(Hyg)*-containing genotypes.

Ds(Hyg) Is Associated with *im-2*

We hypothesized that the *im-2* mutation was caused by the *Ds* insertion. The wild-type phenotype progeny were selected for the presence of *Ds(Hyg)* on hygromycin-containing medium. The presence of 35S::*TPase* in *Ds(Hyg)* hygromycin-resistant lines was monitored. Mutant lines with no 35S::*TPase* gene were further studied as stable mutants for genetic linkage analysis. Lines positively scored for 35S::*TPase* were kept as potentially unstable and were used as a source for revertants.

Genetic linkage of the insertion to the mutation was assessed using the hygromycin resistance gene carried by the modified *Ds(Hyg)* element. All of the 35 lines tested (F_3 from the originally identified plant carrying the mutation) that were heterozygous for the *im-2* mutation were also heterozygous for the *Ds(Hyg)* element. From this result, and because no hygromycin-sensitive lines lacking *Ds(Hyg)* were found to carry the *im-2* mutation, we deduced that the *Ds* element genetically was closely linked to the *im-2* mutation.

A 400-bp DNA fragment flanking *Ds(Hyg)* in the mutant was isolated by inverse polymerase chain reaction (IPCR) (see Methods). When used as a probe in a DNA gel blot hybridization experiment, it detected an extra fragment that was present only in lines carrying *im-2* (Figure 2). From these experiments, we conclude that *im-2* carries a new *Ds* insertion linked to the mutated locus.

To prove that the *Ds* element causes the *im-2* mutation, we looked for reversion events that would correlate the loss of the mutant phenotype with the restoration of a wild-type gene (Coupland, 1992; Walbot, 1992). In the mutant, *Ds(Hyg)* was inserted in an exon (see below). We expected the excision of *Ds(Hyg)* from *im-2* to leave an 8-bp footprint, disrupting the *IM* reading frame. However, rare imprecise or precise excision of *Ds* could restore a functional *IM* gene (Coupland, 1992; Walbot, 1992; Long et al., 1993). *im-2* plants carrying the 35S::*TPase* construct were propagated and examined for large green sectors. Most of the sectors were mutant green sectors, resulting in variegated progeny (as seen in Figure 1A). However, five sectored plants gave rise to progeny segregating for fully green plants. The sequence of the *Ds(Hyg)* insertion site in the stable, full green plants showed that excision of *Ds(Hyg)* from its insertion site left a footprint that restored the coding sequence, leaving a putatively functional IM protein product (Figure 3). From a green sector with a variegated progeny, we identified a line, *im-2d*, that is a variegated mutant derivative of *im-2.* The sequence of the *Ds(Hyg)* insertion point reveals a 2-bp insertion that disrupts the reading frame (Figure 3).

The *IM* locus had been mapped on chromosome 4 of Arabidopsis between the *AGAMOUS* and *CER2* loci in a 9.2-centimorgan (cM) interval (Wetzel et al., 1994). We verified the map position of the *Ds(Hyg)* causing the *im-2* mutation. We found that the *Ds(Hyg)* flanking sequence hybridizes with yeast artificial chromosomes (YACs) CIC5A4, CIC5C2, and CIC7A5 from the CIC library (Creusot et al., 1995). These YACs were mapped previously to the position of markers JBG9 on the chromosome 4 physical map (Lister and Dean, 1993; Schmidt et al., 1995) within the same area at which *im* has been mapped.

Evidence for Tagging of the *IM* Gene

The sequence of the *Ds(Hyg)* flanking fragment did not show any putative open reading frames (ORFs), and neither did it identify any known nucleotide sequence in the database. We used the *Ds(Hyg)* flanking fragment as a probe to isolate a genomic clone containing the corresponding sequence. We characterized a 3.4-kb EcoRI genomic DNA fragment containing the entire *Ds(Hyg)* flanking sequence. The nucle-

otide sequence of the genomic clone revealed a putative ORF and identified two expressed sequence tags (T42793 and AA395166) from Arabidopsis. The entire EcoRI fragment was used to probe a cDNA library. Two clones were isolated and identified a 1.4-kb cDNA containing a putative ORF. Comparison of the genomic and cDNA sequences allowed exon/intron locations on the genomic sequence to be predicted. The *Ds(Hyg)* insertion site was located at the beginning of exon 2, which is 24 bp from the splice junction site, interrupting the coding sequence and duplicating an 8-bp target site, as expected for a *Ds* insertion (Walbot, 1992) (Figures 3 and 4).

During the course of these experiments, we made the EcoRI genomic clone available to others to be used as a probe on a fine physical map of the *IM* region. This probe allowed the identification of the original *im* allele and the *spotty* allele (Wu et al., 1999).

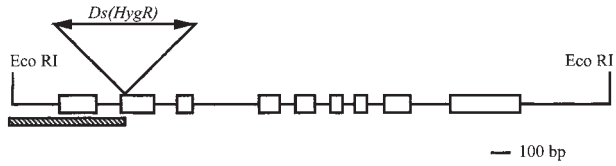

Figure 4. Structure of the *IM* Gene.

Boxes indicate exons, and lines denote noncoding and intron sequences. The *Ds(Hyg)* insertion point, as determined by comparison of the genomic sequence with the nucleotide sequence of the *Ds(Hyg)* DNA obtained by IPCR, is shown. The genomic sequence is entirely contained within the 3.4-kb EcoRI fragment. Nine exons and eight introns have been identified. All exon/intron splice sites follow the GT/AG consensus. The genomic sequence had been determined (EMBL accession number ATT10I14) as part of the sequencing of chromosome 4 of Arabidopsis (Bevan et al., 1998). The striped box indicates the position of the *Ds(Hyg)* flanking sequence used as a probe on DNA gel blot (Figure 2).

Determining the *IM* Coding Sequence

The sequence of the *IM* cDNA shows a putative start codon followed by a 350–amino acid ORF, encoding a putative 40.5-kD protein (Figure 5). A homology search using the BlastP program (Altschul et al., 1997) revealed a weak but significant homology to polypeptides belonging to the mitochondrial alternative oxidase (AOX) protein family. No other significant homology was found. The homologous region starts at amino acid 111 and shows 29% identity (45% similarity) to the soybean AOX. Despite the weak identity with AOX, a computer search for secondary structure and putative domains of biological significance revealed structural similarities between IM and AOX (Figure 6). It is remarkable that transmembrane helix domains found in AOX are located at similar positions on the peptide sequence of IM, suggesting a membrane location for IM and also a configuration in membranes similar to that of AOX. In addition, an iron binding motif was found to be conserved between IM and AOX (Figure 6). Interestingly, the sequence alignments between IM and AOX protein show a 19–amino acid insertion in the IM protein corresponding to parts of exons 7 and 8.

```
A.   CGA GTC CAA GCA ACG ATT TTG CAA GAC GAT GAA GAG AAA GTG
     R   V   Q   A   T   I   L   Q   D   D   E   E   K   V

B.   CGA GTC CAA GCA A (Ds) CCA AGC AAC GAT TTG CAA GAC GAT GAA
     R   V   Q   A

C.   CGA GTC CAA GCA ACG GGA TTT TGC AAG ACG ATG AAG AGA AA GTG
     R   V   Q   A   T   G   F   C   K   T   stop at codon 89

D.   CGA GTC CAA GCA AGG GAA CCA CCA ATT TTG CAA GAC GAT GAA GAG
     R   V   Q   A   R   E   P   P   I   L   Q   D   D   E   E

E.   CGA GTC CAA GCA AGT GAA CCA ACG ATT TTG CAA GAC GAT GAA GAG
     R   V   Q   A   S   E   P   T   I   L   Q   D   D   E   E

F.   CGA GTC CAA GCA AGT GAA CCA ACG ATT TTG CAA GAC GAT GAA GAG
     R   V   Q   A   S   E   P   T   I   L   Q   D   D   E   E

G.   CGA GTC CAA GCA AGT GAA GCA ACG ATT TTG CAA GAC GAT GAA GAG
     R   V   Q   A   S   E   A   T   I   L   Q   D   D   E   E
```

Figure 3. Sequences of Alleles of *IM* Derived from *im-2* by *Ds(Hyg)* Excision.

Green-sectored potentially unstable mutants, with the *Ac* transposase (35S::*TPase*), were selected. DNA from F_1 fully green plants was used as template for PCR amplification encompassing the *Ds(Hyg)* insertion point. PCR was performed using primers on each side of the *Ds(Hyg)* insertion. Bases not present in the wild type are underlined. The amino acid sequence deduced from the DNA sequence is indicated. Sequence A shows the relevant region of the wild-type gene. Sequence B is of the *im-2* allele, and the 8 bp duplicated upon *Ds(Hyg)* insertion are underlined. Sequence C is of a stable *im* allele derived from *im-2* by *Ds(Hyg)* excision. Sequences D to G represent revertant alleles of *IM* derived from *im-2* by *Ds(Hyg)* excision. Sequences D to G show a restoration of the reading frame in their sequences. Sequence C is from a line with a mutant phenotype and was found to carry a 2-bp insertion disrupting the reading frame.

The N terminus of the IM sequence shows the features of a chloroplast transit peptide (von Heijne et al., 1989; Michl et al., 1994). This presequence is common to most nuclear-encoded chloroplast proteins. Structure rather than sequence is responsible for precise routing from the cytoplasm to the chloroplast compartment. The IM putative transit peptide is rich in leucine/arginine and serine/threonine. Computer analysis of the putative transit peptide (Psort software; Nakai and Kanehisa, 1992) suggested a possible targeting of IM to the thylakoid compartment of the chloroplast.

IM Is Associated with the Thylakoids

To confirm that IM was indeed located in the chloroplast, we performed in organello import experiments to test whether the

polypeptide deduced from the cDNA sequence is translated as a precursor with a transit peptide sufficient for chloroplast targeting. After in vitro transcription, the IM protein was in vitro translated in the presence of ^{35}S-methionine. The labeled precursor was identified by SDS-PAGE as a 45-kD protein. When incubated with isolated pea chloroplasts, the precursor is imported into chloroplasts and processed to a 37-kD protein (Figure 7, lanes 1 and 2). The precursor protein is digested by thermolysin, whereas the mature form is protected against digestion (Figure 7, lane 3). This result shows that the IM protein transit peptide targets the IM protein into the chloroplasts. The smaller size of the imported protein is consistent with the cleavage of the transit peptide during protein import.

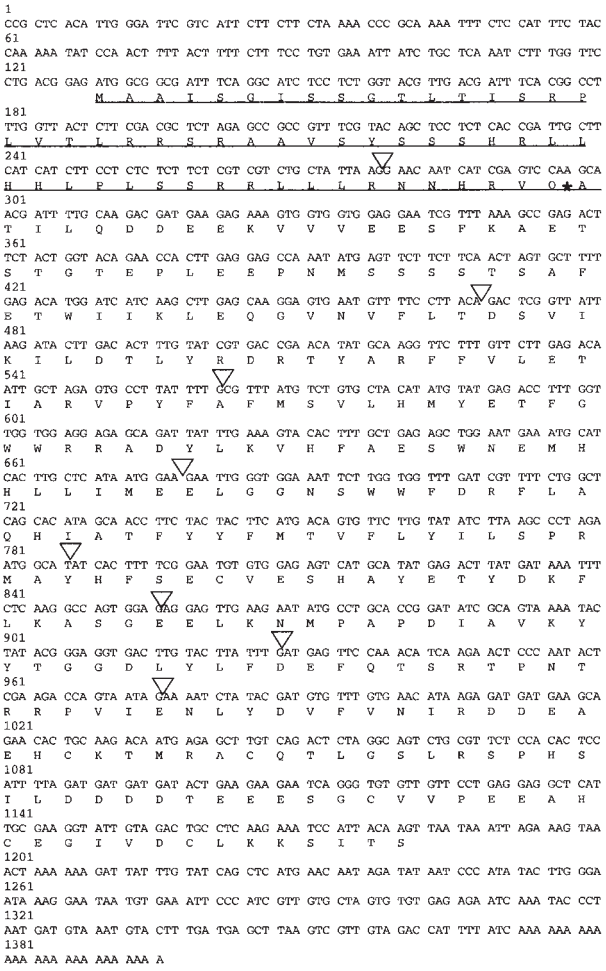

Figure 5. cDNA and Deduced Amino Acid Sequences of IM.

The putative N-terminal chloroplast transit peptide is underlined, with the likely point of cleavage indicated by an asterisk. Open triangles indicate intron positions (EMBL accession number AJ004881).

To obtain further information on the localization of IM within plastids, we fractionated chloroplasts into stroma and thylakoids. The IM protein was found associated with the thylakoid fraction and was not detected in the stroma fraction (Figure 7, lanes 5 and 6). Furthermore, when chloroplasts were lysed before thermolysin treatment, the mature IM protein remained partially resistant to protease attack (Figure 7, lane 4), suggesting a localization inside the thylakoid membranes where the photosynthetic electron transfer occurs.

Detection of the *IM* Transcript

The phenotype conferred by *im-2* together with the location of the IM protein in the chloroplast clearly are related to leaf and chloroplast function. We attempted to detect *IM* mRNA in both photosynthetic and nonphotosynthetic tissues. Reverse transcriptase–PCR (RT-PCR) experiments performed with RNA extracted from Arabidopsis leaves and roots showed a clear difference in the abundance of the PCR products. In RNA from leaves, an intense band corresponding to the 5′ end of *IM* mRNA was obtained. A much less abundant PCR product was also obtained with root RNA, showing the presence of the *IM* transcript in roots as well as in leaves (Figure 8A). Based on the difference observed, we assume that *IM* mRNA is preferentially accumulated in leaves, reflecting the importance of IM in photosynthetic tissues (which accumulate carotenoids). However, detection of the *IM* transcript in roots raises the question of IM function in these nonphotosynthetic tissues (which contain little carotenoids).

RT-PCR performed with RNA extracted from *im-2* plants showing mainly green tissue did not reveal any *IM* mRNA (Figure 8B). Therefore, we can exclude the possibility that green sectors appearing in variegated *im-2* plants are due to the restoration of an *IM* transcript. Genetic and RT-PCR experiments showed that the appearance of green sectors in *im-2* is not a somatic reversion of the mutation. The explanation of the *im*-conferred variegated phenotype must lie in the function of the *IM* gene product and the physiological response of plant cell chloroplasts in its absence (see Discussion).

DISCUSSION

Transposon Tagging of the *IM* Gene

When introduced into the Arabidopsis genome, *Ds* transposition preferentially causes insertional mutations at sites genetically linked to its starting position (Bancroft and Dean, 1993; Machida et al., 1997). The *Ds(Hyg)* element used in this study was initially located on chromosome 4 between markers pCITd71 (1.6 cM) and mi475 (6.4 cM) (Long et al., 1997). These markers are located between *AGAMOUS* and

```
IMM  : 111 FLTDSVIKILDTLYRDRTYA-RFFVLETIARVPYFAFMSVLHMYETFGWWRRADYLKVHF 169
           + T  +++I   L+  R Y  R  +LET+A VP      +LH+     + +   ++K
AOX  : 136 YRTVKLLRIPTDLFFKRRYGCRAMMLETVAAVPGMVGGMLLHLRSLRKFQQSGGWIKALL 195

IMM  : 170 AESWNEMHHLLIMEELGGNSWWFDRFLAQHIATFYYFMTVFLYILSPRMAYHFSECVESH 229
            E+ NE  HL+ M EL     W++R L   +   ++      LYILSP++A+     +E
AOX  : 196 EEAENERMHLMTMVEL-VKPKWYERLLVLAVQGVFFNAFFVLYILSPKVAHRIVGYLEEE 254

IMM  : 230 AYETYDKFLK-ASGEELKNMPAPDIAVKYYTGGDLYLFDEFQTSRTPNTRRPVIENLYDV 288
           A  +Y ++LK      ++N+PAP IA+ Y+                  R P    L DV
AOX  : 255 AIHSYTEYLKDLESGAIENVPAPAIAIDYW------------------RLPKDARLKDV 295

IMM  : 289 FVNIRDDEAEH 299
              IR DEA H
AOX  : 296 ITVIRADEAHH 306
```

Figure 6. Comparison of IM and the Soybean AOX Protein.

(+) indicates similar amino acids. Boxed amino acids are part of predicted transmembrane helix domains. Iron binding motifs present in AOX and IM are indicated by heavy lines below and above the sequences, respectively. Dashes indicate spaces that were introduced to optimize alignment. The soybean sequence has GenBank accession number U87906.

RPS2 loci in a 12- to 13-cM interval. The *IM* locus had been mapped between the *AGAMOUS* and *CER2* loci in a 9.2-cM interval (Wetzel et al., 1994) within the same area. In the case of the variegated albino mutant *im-2* reported here, the *Ds(Hyg)* flanking sequences also have been mapped on YACs in this area. This indicates that the *Ds* insertion is in the *IM* area that is close to the T-DNA from which *Ds(Hyg)* excised. Several lines of evidence indicate that the *IM* gene has been tagged. First, the linkage of the hygromycin resistance gene carried by the *Ds* element to the mutation was demonstrated by a complete lack of recombination between *Ds(Hyg)* and *im-2* for 35 lines tested. Second, revertant alleles of *im-2* were obtained and showed reversion of the phenotype concomitantly with the restoration of the reading frame in the *IM* coding sequence. In addition, the gene identified in this study allowed others (Wu et al., 1999) to isolate the lesion in the original allele of *im.* Furthermore, the allelism tests proved that *im-2* is allelic to the *spotty* allele of *im. im-2* is a tagged, probably null allele of *im.*

Molecular and Physiological Basis for the Variegated Phenotype

The phenotype associated with *im-2* is variegated. It is unlikely that the variegated phenotype is due to leaky or unstable expression of *IM* because all known alleles (including the tagged one) display the same phenotype (Rédei, 1963; Wetzel et al., 1994). In addition, we show that no *IM* transcript can be detected in green sectors of variegated plants.

Accumulation of phytoene in the white areas of *im-2* plants suggests a block of PDS in carotenoid biosynthesis. This blockage does not affect PDS directly because its gene was mapped elsewhere (Wetzel et al., 1994). This block may be only partial, at least in green *im-2* tissues, as shown by the low amount of phytoene and the accumulation of 50% of normal levels of colored carotenoid in these tissues. The variegation is largely dependent on growth conditions, such as light and temperature (Wetzel et al., 1994; data not shown). High light or extreme temperature can cause photooxidative damage in normal plants. Even standard light conditions can trigger photooxidation in carotenoid-deficient plants, for example, after partial block of PDS activity by herbicide treatment, such as norflurazon (Sandmann and Albrecht, 1990). In the latter case, photooxidative damage is usually limited or absent in dim light.

We speculate that the *im* mutation is phenotypically expressed via photooxidation caused by a partial block in PDS activity. In this model, reduced carotenoid synthesis is expected to cause photooxidative damage (white plastids) preferentially under high light conditions. This trend was observed. It also should be mentioned that white sectors (devoid of carotenoids) do not result necessarily from a total block in carotenoid biosynthesis, because carotenoids synthesized previously are likely to be destroyed under photooxidative conditions. Green sectors would originate from mutant cells (lacking IM) that despite their lower carotenoid

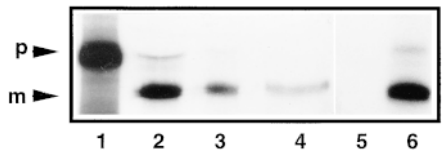

Figure 7. Import of the IM Precursor Protein into Isolated Pea Chloroplasts.

Pea chloroplasts were incubated in vitro with the radiolabeled IM precursor protein. After incubation, chloroplasts were repurified and lysed hypotonically. Proteins were analyzed by SDS-PAGE and subjected to fluorography. Lane 1 contains protein before import; lane 2, protein after import reaction; lane 3, protein from repurified thermolysin-treated chloroplasts; lane 4, protein after import, lysis of the chloroplasts, and thermolysin treatment; lane 5, stromal fraction after import; and lane 6, membrane fraction after import. p, precursor protein; m, mature protein.

biosynthetic content, could avoid irreversible photooxidative damage. This is enhanced in permissive conditions, such as low light, when lower carotenoid levels are sufficient. In summary, in this model the IM protein is a cofactor for phytoene desaturation but is dispensable. When the IM protein is present, the PDS reaction is efficient. When IM is absent or not functional, PDS activity is reduced, and carotenoids accumulate slowly within the plastids, possibly by a mechanism involving the photosynthetic electron transport chain (see below), as proposed by Norris et al. (1995).

This model also takes into account the suggestion by Röbbelen (1968) that IM is active during a discreet light-responsive phase of plant development. In fact, early phases of normal chloroplast formation are characterized by upregulation of carotenoid biosynthesis (Corona et al., 1996) to cover the need for de novo photosystem assembly and for protection against photooxidation (which could occur in partially assembled photosystems and/or because of the presence of photoreactive chlorophyll biosynthesis intermediates). Furthermore, during these stages, the presence of IM may be crucial because the IM-independent phytoene desaturation pathway (photosynthetic electron transfer chain) may not be fully functional. Consequently, IM can be considered to be an essential protein during the early stages of chloroplast differentiation.

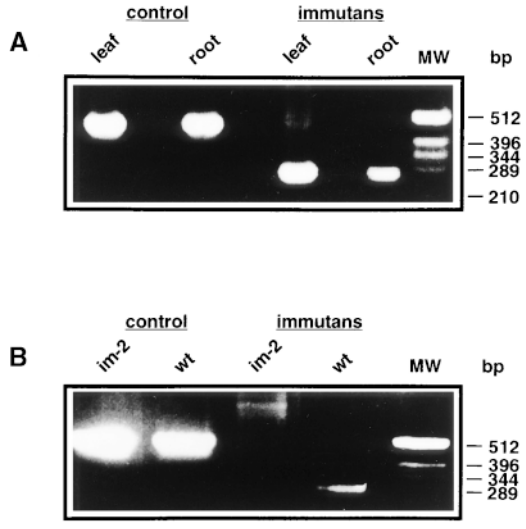

Figure 8. Detection of *IM* mRNA by RT-PCR.

(A) Detection of *IM* mRNA in leaf and root mRNA. Agarose gel analysis was conducted with RT-PCR products obtained after PCR. Control, primers specific to the *ADENINE PHOSPHORIBOSYL TRANSFERASE* control gene; immutans, primers Dave6 and Dave5 specific for *IM*; MW, molecular mass markers; bp, lengths of molecular mass markers in base pairs.

(B) Detection of *IM* mRNA in wild-type (wt) but not in the *Ds(Hyg)*-tagged allele (im-2). In both RT-PCR experiments, the expected size of PCR fragment was obtained. MW and bp are as given in **(A)**.

Functional Role of IM

The sequence similarity between IM and AOX enable the prediction of an enzymatic function for IM. AOX is an iron-dependent enzyme, and iron deficiency has been shown to block carotene desaturation at the level of phytoene desaturation (Pascal et al., 1995). It is striking that an iron binding motif is also present in IM (Figure 6). AOX is found in plant mitochondria, where it is responsible for an oxidative cyanide–insensitive pathway, bypassing the cytochrome (cyanide-sensitive) respiratory electron transfer chain (Siedow and Umbach, 1995; Vanlerberghe and McIntosh, 1997). AOX can oxidize the ubiquinone pool and uses molecular oxygen as a terminal acceptor. Interestingly, quinone involvement in phytoene desaturation is indicated by the fact that phytoene desaturation is impaired when bleaching cyclohexanedione herbicides (which inhibit the enzyme *p*-hydroxyphenylpyruvate dioxygenase in the quinone biosynthesis pathway) are applied to plants (Schultz et al., 1993) or when the gene for this enzyme is inactivated by mutation (Norris et al., 1995). In addition, molecular oxygen also has been proposed to be essential for carotene desaturation, at least in nonphotosynthetic plastids (Beyer et al., 1989).

Taking into account these data and the fact that after import into chloroplasts IM is located in thylakoids, which also contain the photosynthetic electron transfer chain and PDS (Linden et al., 1993), we predict that the IM protein is involved in electron transfer associated with phytoene desaturation, namely, the reoxidation of plastoquinol to plastoquinone, using oxygen as a terminal acceptor. In this model (Figures 9A and 9B), the IM protein would act as a terminal oxidase, and its activity would parallel that of the photosynthetic electron transfer chain.

Quinones are intermediate electron acceptors in phytoene desaturation because PDS uses flavin adenine dinucleotide (Al-Babili et al., 1996) or NADP as a cofactor (Fraser et al., 1993). Whether IM also participates in the redox reactions involving these cofactors or whether this part of the whole desaturation process is fulfilled by a separate redox protein is not known. In fact, such a redox protein (a NADPH:quinone oxidoreductase) has been described in nonphotosynthetic plastids (Nievelstein et al., 1995). However, in this study, the latter redox protein is assumed to function differently, namely, in a coreduction-like mechanism that could provide the driving force of the desaturation reaction. Our model may therefore be oversimplified and will be extended when the additional redox compounds have been identified.

Although the models represented in Figures 9A and 9B do not show IM and PDS in close association, we do not exclude this possibility; neither do we exclude the fact that IM itself could be mechanistically involved in the process, providing the driving force for the reaction. The latter possibility might explain why carotenoid desaturation is also limited in green sectors of *im* plants, although the photosynthetic electron transfer chain capacity to reoxidize plastoquinone is obviously vastly greater than is the amount of plastoquinol

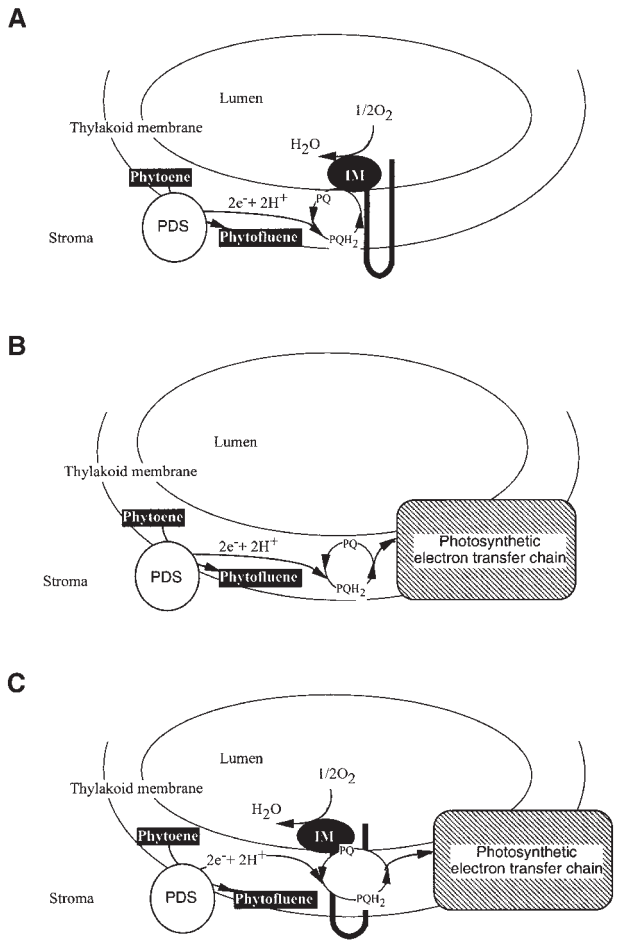

Figure 9. Model for the Action of IM in Chloroplast Carotenoid Biosynthesis.

(A) In wild-type plants, phytoene desaturation involves plastoquinones (PQ/PQH_2) as electron acceptors. In this model, IM would be a terminal oxidase transferring electrons from reduced plastoquinones to soluble oxygen, forming water.

(B) In the absence of IM, in mutant plants, reoxidation of PQH_2 produced by PDS activity cannot involve oxygen. Electrons can be transferred via the photosynthetic electron transfer chain. This step would be rate limiting or inefficient in the early stages of chloroplast differentiation due to the absence of organized thylakoid membranes. Chloroplasts in *im* plants would be prone to photooxidation under high light conditions because carotenoid biosynthesis is not sufficient. Under low light conditions, enough carotenoids might be produced to protect the developing chloroplast.

(C) In this model, IM would act in closer association with PDS and would facilitate its activity (possibly as part of a mechanism providing the driving force of the reaction) in both nonphotosynthetic and photosynthetic tissues. In the latter case, both the electron transport chain and the oxygen pathways could be used in the presence of IM. In the absence of IM, PDS activity would become inefficient even in green tissues.

produced by carotenoid desaturation. IM could facilitate the reaction in wild-type green tissues by using plastoquinones as a cofactor, which either could be directly reoxidized using molecular oxygen or, after being released, could be reoxidized efficiently by the photosynthetic chain. In such a version of our model (Figure 9C), both pathways could be functional in green organs from wild-type plants and involve IM.

We conclude from both in vitro import experiments and computer analysis of its transit peptide that IM is located in the thylakoids. However, we do not rule out the possibility that IM may also be present to some extent in the plastid envelope. The latter possibility might be of physiological importance in nonphotosynthetic tissues, such as those of roots in which *IM* transcripts have been detected. In these tissues, carotenoids may serve as precursors for abscisic acid (Tan et al., 1997).

The accumulation of phytoene in mutant cells indicates that IM is a cofactor for the first desaturation step (phytoene to phytofluene), as shown in Figure 9. It seems likely that it also participates in the second step (phytofluene to ζ-carotene), which also is catalyzed by PDS, and also may be involved in the following two steps (ζ-carotene to neurosporene and lycopene), which are catalyzed by a distinct but similar desaturase (Albrecht et al., 1995). The latter possibility remains to be demonstrated.

Our model also may be extended to incorporate additional electron transport mechanisms, such as chlororespiration. Chlororespiration, the uptake of oxygen (respiration) by chloroplasts in the dark (Bennoun, 1982), may require oxidation of the plastoquinone pool by oxygen (Feild et al., 1998). This mechanism might involve the plastid-encoded NDH polypeptides, which are subunits of the NADH:ubiquinone oxido-reductase complex (Burrows et al., 1998), and an uncharacterized terminal oxidase. It remains to be investigated whether, in addition to its role in PDS activity, IM also might have a more ubiquitous terminal oxidase activity. If this assumption is correct, chloroplasts from the *im-2* mutant and other null alleles of *IM* should be impaired in chlororespiration.

METHODS

Plant Growth Conditions

The *Arabidopsis thaliana* Landsberg *erecta* line carrying the *Activator* (*Ac*) transposase gene fused to the cauliflower mosaic virus 35S promoter (35S::*TPase*) was described previously (Swinburne et al., 1992). The Arabidopsis line carrying Tn*113* and harboring *Ds(Hyg)* has been described previously (Long et al., 1993), and the T-DNA insertion carrying the *Ds(Hyg)* transposon was mapped on chromosome 4 at 2.9 centimorgans (cM) below the *AGAMOUS* locus (Long et al., 1997). Detection of the T-DNA carrying the 35S::*TPase* construct was done by detecting β-glucuronidase (GUS) activity associated with 35S::GUS (Long et al., 1993). Antibiotic selection of *Ds(Hyg)*, namely, hygromycin resistance and streptomycin resistance associated

with *Dissociation* (*Ds*) excision from the T-DNA (Coupland, 1992), was described by Long et al. (1993).

Determination of Carotenoid Content

Freeze-dried material (aerial parts of Arabidopsis) was extracted with methanol containing 6% KOH at 60°C for 20 min. Carotenoids were partitioned into 10% ether in petrol, evaporated to dryness, redissolved in acetone, and analyzed by HPLC. HPLC analysis was performed on a Nucleosil C18, 35-mm column (Machery-Nagel, Duren, Germany) by using acetonitrile–methanol–2-propanol (85:10:5 [v/v]) and a flow of 1 mL/min. Absorbance was at 285 and 440 nm, and spectra were recorded with a diode array detector (model 440; Kontron Instruments, Neufarm, Germany). Identification and quantitation were performed using standards and the extinction coefficient listed by Davis (1976).

DNA and RNA Gel Blot Analyses

Isolation of Arabidopsis DNA was performed as described previously (Sundaresan et al., 1995). The DNA gel blot was probed with the *Ds* flanking sequence isolated from an agarose gel radioactively labeled by random priming using ^{32}P-dCTP (Sambrook et al., 1989) and exposed to Kodak x-ray film (Eastman Kodak). The genomic library of Arabidopsis Landsberg *erecta gai* DNA has been described by Whitelam et al. (1993). Screening the library was performed using the plaque lift method (Sambrook et al., 1989). Approximately 100,000 phage plaques were screened using the ^{32}P-dCTP radiolabeled–*Ds* flanking sequence. Positive clones were further purified, and the 3.4-kb EcoRI DNA fragment containing the *IMMUTANS* (*IM*) gene was isolated, subcloned into pBluescript KS+ (Stratagene, La Jolla, CA), and sequenced using the chain termination method.

To isolate cDNA clones, an Arabidopsis cDNA library (Stratagene) was screened using the colony lift method (Sambrook et al., 1989). Approximately 300,000 colonies were plated and screened for the presence of the *IM* cDNA. Positive clones were further purified and sequenced.

Inverse polymerase chain reaction (IPCR) was used to isolate the DNA flanking the *Ds(Hyg)* element. Two micrograms of DNA from plants heterozygous for the *im-2* mutation was cleaved with BstyI and subjected to IPCR according to Long et al. (1993). The primers used to amplify the *Ds* flanking sequence described in this study were D73 and E4 (Long et al., 1993). The PCR product was cloned into a plasmid vector, propagated in *Escherichia coli,* and sequenced.

To isolate DNA from revertants, PCR was performed using the primers Dave6 (5′-GTTCCTGACGGAGATGGC-3′) and IM03 (5′-GTCCCTGACGGAGATGGC-3′) with 10 ng of plant DNA as template, followed by 4 min of denaturation at 94°C and 30 cycles of amplification (1 min at 94°C, 1 min at 53°C, and 1 min at 72°C). The PCR product was purified and sequenced using the PCR sequencing method with the same primers.

Plant RNA was extracted from 100 mg of fresh tissues. Plant tissues were ground in Eppendorff tubes containing 300 μL of extraction buffer as described previously (Cowling et al., 1998). Reverse transcription followed by PCR (RT-PCR) detection of the *IM* transcript were performed with 1 to 3 μg of RNA, according to Cowling et al. (1998). Primers used for RT-PCR were Dave6 (see above) and Dave5 (5′-GAACTCATATTTGGTTCC-3′). Control primers to amplify the *ADENINE PHOSPHORIBOSYL TRANSFERASE* gene (Moffatt et al., 1994) and PCR conditions are described by Cowling et al. (1998).

Sequence comparison was performed using Internet resources. Prediction of thylakoid transit peptide for the N-terminal part of *IM* was performed using Psort software located at the Institute for Molecular and Cellular Biology (Osaka University, Osaka, Japan) (http://psort.nibb.ac.jp:8800/). Transmembrane helix prediction was performed at the Center for Biological Sequence Analysis (Technical University of Denmark) (http://www.cbs.dtu.dk/services/TMHMM-1.0/). Sequence alignment was performed using the BlastP program from the NCBI Internet site (http://www.ncbi.nlm.nih.gov/cgi-bin/BLAST/nph-newblast).

Isolation of Chloroplasts, Production of Precursor Protein, and Import Reactions

Chloroplasts were isolated from 10- to 12-day-old pea seedlings (*Pisum sativum* var Petit Provençal) as described by Waegemann and Soll (1995) and suspended in import buffer (50 mM Hepes-KOH, pH 7.6, and 330 mM sorbitol) at a concentration of 1 mg of chlorophyll per mL.

The plasmid containing the complete cDNA was linearized with the restriction enzyme XhoI and transcribed into mRNA using T7 RNA polymerase following the protocol of the manufacturer (Promega). Translation of the resulting mRNA was conducted in the presence of ^{35}S-methionine (Amersham) in a rabbit reticulocyte lysate system as recommended by the supplier (Promega).

Chloroplast protein import reactions were performed as described by Weagemann and Soll (1995). After import, half of the samples were treated with 200 μg/mL of thermolysin (Sigma) before SDS-PAGE analysis of the proteins and fluorography.

ACKNOWLEDGMENTS

We thank Jean-Pierre Alcaraz for DNA sequencing; Gerard Clabault for his expert computer and DNA analysis; Mireille Rocipon for photographs and help in preparing documents for publication; Gaynor Green for checking the manuscript; Thierry Lagrange, Gilles Vachon, and Jean-Gabriel Valay for critical reading and comments on the manuscript; Nick Harberd for laboratory space and use of the genomic library; Jean-Gabriel Valay and Silva Mache for the cDNA library; and Rachel Cowling for her constant support.

Received July 24, 1998; accepted November 3, 1998.

REFERENCES

Al-Babili, S., Von Lintig, J., Haubruck, H., and Beyer, P. (1996). A novel, soluble form of phytoene desaturase from *Narcissus pseudonarcissus* chromoplasts is Hsp70-complexed and competent for flavinylation, membrane association and enzymatic activation. Plant J. **9,** 601–612.

Albrecht, M., Klein, A., Hugueney, P., Sandmann, G., and Kuntz, M. (1995). Molecular cloning and functional expression in *E. coli*

of a novel plant enzyme mediating ζ-carotene desaturation. FEBS Lett. **372,** 199–202.

Altschul, S.F., Madden, T.L., Schaffer, A.A., Zhang, J., Zhang, Z., Miller, W., and Lipman, D.J. (1997). Gapped BLAST and PSI-BLAST: A new generation of protein database search programs. Nucleic Acids Res. **25,** 3389–3402.

Bancroft, I., and Dean, C. (1993). Transposition pattern of the maize element *Ds* in *Arabidopsis thaliana.* Genetics **134,** 1221–1229.

Bartley, G.E., Vitanen, P.V., Pecker, I., Chamovitz, D., Hirschberg, J., and Scolnik, P.A. (1991). Molecular cloning and expression in photosynthetic bacteria of a soybean cDNA coding for phytoene desaturase, an enzyme of the carotenoid biosynthetic pathway. Proc. Natl. Acad. Sci. USA **88,** 6532–6536.

Bennoun, P. (1982). Evidence for a respiratory chain in the chloroplast. Proc. Natl. Acad. Sci. USA **79,** 4352–4356.

Bevan, M., et al. (1998). Analysis of 1.9 Mb of contiguous sequence from chromosome 4 of *Arabidopsis thaliana.* Nature **391,** 485–488.

Beyer, P., Mayer, M.P., and Kleinig, H. (1989). Molecular oxygen and the state of geometric isomerism of intermediates are essential in the carotene desaturation and cyclization reactions in daffodil chromoplasts. Eur. J. Biochem. **184,** 141–150.

Bilang, R., and Bogorad, L. (1996). Light-dependent developmental control of *rbcS* gene expression in epidermal cells of maize leaves. Plant Mol. Biol. **31,** 831–841.

Bramley, P.M. (1997). Isoprenoid metabolism. In Plant Biochemistry, P.M. Dey and J.B. Harborne, eds (San Diego, CA: Academic Press), pp. 417–437.

Burrows, P.A., Sazanov, L.A., Svab, Z., Maliga, P., and Nixon, P.J. (1998). Identification of a functional respiratory complex in chloroplasts through analysis of tobacco mutants containing disputed plastid *ndh* genes. EMBO J. **17,** 868–876.

Chatterjee, M., Sparvoli, S., Edmunds, C., Garosi, P., Findlay, K., and Martin, C. (1996). *DAG*, a gene required for chloroplast differentiation and palisade development in *Antirrhinum majus.* EMBO J. **15,** 4194–4207.

Chory, J., and Susek, R.E. (1994). Light signal transduction and the control of seedling development. In *Arabidopsis*, E.M. Meyerowitz and C.R. Somerville, eds (Cold Spring Harbor, NY: Cold Spring Harbor Laboratory Press), pp. 579–614.

Corona, V., Aracri, B., Kosturkova, G., Bartley, G.E., Pitto, L., Giorgetti, L., Scolnik, P.A., and Giuliano, G. (1996). Regulation of a carotenoid biosynthesis gene promoter during plant development. Plant J. **9,** 505–512.

Coupland, G. (1992). Transposon tagging in *Arabidopsis.* In Methods in *Arabidopsis* Research, C. Koncz, N.-H. Chua, and J. Schell, eds (Singapore: World Scientific), pp. 290–310.

Cowling, R.J., Kamiya, Y., Seto, H., and Harberd, N.P. (1998). Gibberellin dose–response regulation of *GA4* gene transcript levels in *Arabidopsis thaliana.* Plant Physiol. **117,** 1195–1203.

Creusot, F., Fouilloux, E., Dron, M., Lafleuriel, J., Picard, G., Billault, A., LePaslier, D., Cohen, D., Chaboute, M., Durr, A., Fleck, J., Gigot, C., Camilleri, C., Bellini, C., Caboche, M., and Bouchez, D. (1995). The CIC library: A large insert YAC library for genome mapping in *Arabidopsis thaliana.* Plant J. **8,** 763–770.

Davis, B.H. (1976). Carotenoids. In Biochemistry of Plant Pigments, Vol. 2, T.W. Goodwin, ed (London: Academic Press), pp. 38–165.

Feild, T.S., Nedbal, L., and Ort, D.R. (1998). Nonphotochemical reduction of the plastoquinone pool in sunflower leaves originates from chlororespiration. Plant Physiol. **116,** 1209–1218.

Fraser, P.D., Linden, H., and Sandmann, G. (1993). Purification and reactivation of recombinant *Synechococcus* phytoene desaturase from an overexpressing strain of *Escherichia coli.* Biochem. J. **291,** 687–692.

Han, C.D., Coe, E.H., Jr., and Martienssen, R.A. (1992). Molecular cloning and characterisation of *iojap* (*ij*), a pattern striping gene of maize. EMBO J. **11,** 4037–4046.

Hudson, A., Carpenter, R., Doyle, S., and Coen, E.S. (1993). *Olive*: A key gene required for chlorophyl biosynthesis in *Antirrhinum majus.* EMBO J. **12,** 3711–3719.

Inada, H., Kusumi, K., Nishimura, M., and Iba, K. (1996). Specific expression of the chloroplast gene for RNA polymerase (*rpoB*) at an early stage of leaf development in rice. Plant Cell Physiol. **37,** 229–232.

Keddie, J.S., Carroll, B., Jones, J.D., and Gruissem, W. (1996). The *DCL* gene of tomato is required for chloroplast development and palisade cell morphogenesis in leaves. EMBO J. **16,** 4208–4217.

Linden, H., Lucas, M.M., de Felipe, M.R., and Sandmann, G. (1993). Immunogold localization of phytoene desaturase in higher plant chloroplasts. Physiol. Plant. **88,** 229–236.

Lister, C., and Dean, C. (1993). Recombinant inbred lines for mapping RFLP and phenotypic markers in *Arabidopsis thaliana.* Plant J. **4,** 745–750.

Long, D., Martin, M., Sundberg, E., Swinburne, J., Puangsomlee, P., and Coupland, G. (1993). The maize transposable element system *Ac*/*Ds* as a mutagen in *Arabidopsis*: Identification of an *albino* mutation induced by *Ds* insertion. Proc. Natl. Acad. Sci. USA **90,** 10370–10374.

Long, D., Goodrich, J., Wilson, K., Sundberg, E., Martin, M., Puangsomlee, P., and Coupland, G. (1997). *Ds* elements on all five *Arabidopsis* chromosomes and assessment of their utility for transposon tagging. Plant J. **11,** 145–148.

Machida, C., Onouchi, H., Koizumi, J., Hamada, S., Semiarti, E., Torikai, S., and Machida, Y. (1997). Characterization of the transposition pattern of the *Ac* element in *Arabidopsis thaliana* using endonuclease I-*Sce*I. Proc. Natl. Acad. Sci. USA **94,** 8675–8680.

Mandel, M.A., Feldmann, K.A., Herrera-Estrella, L., Rocha-Sosa, M., and Leon, P. (1996). *CLA1*, a novel gene required for chloroplast development, is highly conserved in evolution. Plant J. **9,** 649–658.

Marin, E., Nussaume, L., Quesada, A., Gonneau, M., Sotta, B., Hugueney, P., Frey, A., and Marion-Poll, A. (1996). Molecular identification of zeaxanthin epoxidase of *Nicotiana plumbaginifolia*, a gene involved in abscisic acid biosynthesis and corresponding to the *ABA* locus of *Arabidopsis thaliana.* EMBO J. **15,** 2331–2342.

Martínez-Zapater, J.M., Gil, P., Capel, J., and Somerville, C.R. (1992). Mutations at the Arabidopsis *CHM* locus promote rearrangements of the mitochondrial genome. Plant Cell **4,** 889–899.

Michl, D., Robinson, C., Shackleton, J.B., Herrman, R.G., and Klosgen, R.B. (1994). Targeting of proteins to the thylakoids by bipartite presequences: CF0II is imported by a novel, third pathway. EMBO J. **6,** 1310–1317.

Moffatt, B.A., McWhinnie, E.A., Agarwal, S.K., and Schaff, D.A. (1994). The adenine phosphoribosyltransferase–encoding gene of *Arabidopsis thaliana.* Gene **143,** 211–216.

Mullet, J.E. (1988). Chloroplast development and gene expression. Annu. Rev. Plant Physiol. Plant Mol. Biol. **39,** 475–502.

Nakai, K., and Kanehisa, M. (1992). A knowledge base for predicting protein localization sites in eukaryotic cells. Genomics **14,** 897–911.

Nievelstein, V., Vandekerckhove, J., Tadros, M.H., von Lintig, J., Nitschke, W., and Beyer, P. (1995). Carotene desturation is linked to a respiratory redox pathway in *Narcissus pseudonarcissus* chromoplast membranes: Involvement of a 23-kDa oxygene-evolving-complex-like protein. Eur. J. Biochem. **233,** 864–872.

Norris, S.R., Barrette, T.R., and DellaPenna, D. (1995). Genetic dissection of carotenoid synthesis in Arabidopsis defines plastoquinone as an essential component of phytoene desaturation. Plant Cell **7,** 2139–2149.

Pascal, N., Block, M.A., Pallet, K.E., Joyard, J., and Douce, R. (1995). Inhibition of carotenoid biosynthesis in sycamore cells deprived of iron. Plant Physiol. Biochem. **33,** 97–104.

Pogson, B., McDonald, K.A., Truong, M., Britton, G., and DellaPenna, D. (1996). Arabidopsis carotenoid mutants demonstrate that lutein is not essential for photosynthesis in higher plants. Plant Cell **8,** 1627–1639.

Rédei, G.P. (1963). Somatic instability caused by a cysteine-sensitive gene in *Arabidopsis.* Science **139,** 767–769.

Reiter, R.S., Coomber, S.A., Bourett, T.M., Bartley, G.E., and Scolnik, P.A. (1994). Control of leaf and chloroplast development by the Arabidopsis gene *pale cress.* Plant Cell **6,** 1253–1264.

Röbbelen, G. (1968). Genbedingte Rotlicht-Empfindlichkeit der Chloroplastendifferenzierung bei *Arabidopsis.* Planta **80,** 237–254.

Sakamoto, W., Kondo, H., Murata, M., and Motoyoshi, F. (1996). Altered mitochondrial gene expression in a maternal distorted leaf mutant of Arabidopsis induced by *chloroplast mutator.* Plant Cell **8,** 1377–1390.

Sambrook, J., Fritsch, E.F., and Maniatis, T. (1989). Molecular Cloning: A Laboratory Manual. (Cold Spring Harbor, NY: Cold Spring Harbor Laboratory Press).

Sandmann, G., and Albrecht, M. (1990). Accumulation of colorless carotenes and derivatives during interaction of bleaching herbicides with phytoene desaturation. Z. Naturforsch. **45C,** 487–491.

Schmidt, R., West, J., Love, K., Lenehan, Z., Lister, C., Thompson, H., Bouchez, D., and Dean, C. (1995). Physical map and organization of *Arabidopsis thaliana* chromosome 4. Science **270,** 480–483.

Schultz, A., Ort, O., Beyer, P., and Kleinig, H. (1993). SC-0051, a 2-benzoyl-cyclohexane-1,3-dione bleaching herbicide, is a potent inhibitor of the enzyme *p*-hydroxyphenylpyruvate dioxygenase. FEBS Lett. **318,** 162–166.

Siedow, J.N., and Umbach, A.L. (1995). Plant mitochondrial electron transfer and molecular biology. Plant Cell **7,** 821–831.

Sundaresan, V., Springer, P., Volpe, T., Haward, S., Jones, J.D., Dean, C., Ma, H., and Martienssen, R. (1995). Patterns of gene action in plant development revealed by enhancer trap and gene trap transposable elements. Genes Dev. **9,** 1797–1810.

Sundberg, E., Slagter, J.G., Fridborg, I., Cleary, S.P., Robinson, C., and Coupland, G. (1997). *ALBINO3*, an Arabidopsis nuclear gene essential for chloroplast differentiation, encodes a chloroplast protein that shows homology to proteins present in bacterial membranes and yeast mitochondria. Plant Cell **9,** 717–730.

Swinburne, J., Balcells, L., Scofield, S.R., Jones, J.D.G., and Coupland, G. (1992). Elevated levels of *Activator* transposase mRNA are associated with high frequencies of *Dissociation* excision in Arabidopsis. Plant Cell **4,** 583–595.

Tan, B.C., Schwartz, S.H., Zeevaart, J.A.D., and McCarty, D.R. (1997). Genetic control of abscisic acid biosynthesis in maize. Proc. Natl. Acad. Sci. USA **94,** 12235–12240.

Taylor, W.C. (1989). Regulatory interactions between nuclear and plastid genomes. Annu. Rev. Plant Physiol. Plant Mol. Biol. **40,** 211–233.

Vanlerberghe, G.C., and McIntosh, L. (1997). Alternative oxidase: From gene to function. Annu. Rev. Plant Physiol. Plant Mol. Biol. **48,** 703–734.

von Heijne, G., Steppuhn, J., and Herrmann, R.G. (1989). Domain structure of mitochondrial and chloroplast targeting peptides. Eur. J. Biochem. **180,** 535–545.

Waegemann, K., and Soll, J. (1995). Characterization and isolation of the chloroplast protein import machinery. In Methods in Cell Biology, Vol. 50, D.W. Galbraith, D.P. Bourque, and H.J. Bohnert, eds (New York: Academic Press), pp. 255–268.

Walbot, V. (1992). Strategies for mutagenesis and gene cloning using transposon tagging and T-DNA insertional mutagenesis. Annu. Rev. Plant Physiol. Plant Mol. Biol. **43,** 49–92.

Wetzel, C.M., Jiang, C.-Z., Meehan, L.J., Voytas, D.F., and Rodermel, S.R. (1994). Nuclear-organelle interactions: The *immutans* variegation mutant of *Arabidopsis* is plastid autonomous and impaired in carotenoid biosynthesis. Plant J. **6,** 161–175.

Whitelam, G.C., Johnson, E., Peng, J., Carol, P., Anderson, M.L., Cowl, J.S., and Harberd, N.P. (1993). Phytochrome A null mutants of Arabidopsis display a wild-type phenotype in white light. Plant Cell **5,** 757–768.

Wu, D., Wright, D.A., Wetzel, C., Voytas, D.F., and Rodermel, S. (1999). The *IMMUTANS* variegation locus of Arabidopsis defines a mitochondrial alternative oxidase homolog that functions during early chloroplast biogenesis. Plant Cell **11,** 43–55.